

Evolution of swelling pressure of cohesive-frictional, rough and elasto-plastic granulates

Stefan Luding¹, Erich Bauer^{2*}

¹Multi Scale Mechanics, TS, CTW, UTwente, P.O.Box 217, 7500 AE Enschede, Netherlands

²Institute of Applied Mechanics, Graz University of Technology, A-8010 Graz, Austria

Abstract: The subject of this study is the modeling of the evolution of the swelling pressure of granulates with cohesive-frictional, rough and elasto-plastic “microscopic” contact properties. The spherical particles are randomly arranged in a periodic cubic space with a fixed volume so that an increase of the particle size – i.e. swelling that can be caused by intake of some fluid – is accompanied by a decrease of the void space. An analytical function is proposed that properly describes the (macroscopic) void ratio as function of pressure for different microscopic contact properties.

Keywords: granular materials, discrete element model (DEM), force-laws, friction, rolling- and torsion resistance, adhesion, elasto-plastic deformation

1 Introduction

The evolution of the swelling pressure of a system of discrete particles is the subject of this study. Particles can change size due to a temperature change (which does not change their mass); however, the swelling considered here can be due to intake of a fluid with the corresponding mass-increase. Fine cohesive-frictional, rough particles, e.g. (Tomas 2000), are arranged in a cubic space with fixed volume and then simulated using a discrete element model, e.g. (Rapaport 1995), (Thornton 2000), (Thornton et al. 2001), (Luding et al. 2005), (Luding 2008). The void space between the solid grains is assumed to be empty. The process of swelling is modeled by a constant, finite relative growth rate that leads to an exponential increase of the diameter of the spherical particles with time, up to a state where a target volume fraction is reached. Alternative laws for the growth rate are possible, but not investigated in this paper. As the volume of the specimen is

* corresponding author, email: erich.bauer@tugraz.at

kept constant while the solid grains continuously increase the void space between the particles decreases, which is accompanied by an increase of the average contact pressure, e.g. (Bartels et al. 2005), (Oquendo et al. 2009). In the early stages of swelling the number of contacts increases rapidly and a reorientation of particles within the grain skeleton can take place, e.g. (Morgeneyer et al. 2006). The reorientation of particles and consequently the compaction behavior is also influenced by the pressure level, the particle properties and the contact laws. The present simulations are based on the contact models in the papers by Luding et al. (2005) and Luding (2008). It is also discussed in this paper that the semi-logarithmic representation of the compaction curve shows a soft wave with two regimes, which can be well fitted by the sum of two exponential functions proposed by Bauer (2010).

2 Discrete Particle Model

Particle simulations are referred to as discrete element models. If all forces \mathbf{f}_i acting on the particle i either from other particles, from boundaries or from external forces, are known, the problem is reduced to the integration of Newton's equations of motion for the translational and rotational degrees of freedom:

$$\frac{d}{dt}(m_i \dot{\mathbf{r}}_i) = \mathbf{f}_i + m_i \mathbf{g} \quad \text{and} \quad \frac{d}{dt}(I_i \boldsymbol{\omega}_i) = \mathbf{q}_i \quad (1)$$

with the mass m_i of particle i , its position \mathbf{r}_i , the velocity $\dot{\mathbf{r}}_i$ of the center of mass, the resultant force $\mathbf{f}_i = \sum_c \mathbf{f}_i^c$ acting on it due to contacts with other particles or with the walls, the acceleration due to volume forces like gravity \mathbf{g} , the particles moment of inertia I_i , its angular velocity $\boldsymbol{\omega}_i$ and the resultant torque \mathbf{q}_i . In the following the contact laws used in the present study are briefly outlined for modeling normal interactions, like adhesion and elasto-plastic contact deformations as well as for modeling friction, rolling- and torsion resistance in tangential direction.

Two spherical particles i and j , with radii a_i and a_j , respectively, interact only if they are in contact so that their overlap $\delta = (a_i + a_j) - (\mathbf{r}_i - \mathbf{r}_j) \cdot \mathbf{n}$ is positive, i.e. $\delta > 0$, with the unit vector $\mathbf{n} = \mathbf{n}_{ij} = (\mathbf{r}_i - \mathbf{r}_j) / |\mathbf{r}_i - \mathbf{r}_j|$ pointing from j to i . The force on particle i , from particle j , at contact c , can be decomposed into a normal and a tangential part as $\mathbf{f}^c := \mathbf{f}_i^c = f^n \mathbf{n} + f^t \mathbf{t}$, where $\mathbf{n} \cdot \mathbf{t} = 0$. The tangential force leads to a torque as well as rolling and torsion, as discussed below.

The simplest normal contact force model, which takes into account excluded volume and dissipation, involves a linear repulsive and a linear dissipative force $f^n = k\delta + \gamma_0 v_n$ with a spring stiffness k , a viscous damping γ_0 , and the relative velocity in normal direction $v_n = -\mathbf{v}_{ij} \cdot \mathbf{n} = -(\mathbf{v}_i - \mathbf{v}_j) \cdot \mathbf{n} = \dot{\delta}$. Here a variant of the linear hysteretic spring model is applied, e.g. (Luding et al. 2005), (Luding 2008) as an alternative to the frequently applied spring-dashpot models. This model is

the simplest version of some more complicated nonlinear-hysteretic force laws, which reflect the fact that at the contact point, plastic deformations may take place and attractive (adhesive) forces exist. The elasto-plastic model with contact-adhesion involves three stiffnesses: (i) the plastic k_1 , (ii) the maximal elastic k_2 , and (iii) the adhesion k_c , where the latter determines the strength of the attractive forces. The elasto-plastic range, with stiffness and adhesion dependent on the preloading, is active for small overlaps with relative overlap smaller than ϕ_f . For stronger deformations, the particles behave linearly elastic with stiffness k_2 . For details see Luding et al. (2005) and Luding (2008). For the sake of simplicity, the medium range van der Waals forces that also can be taken into account are disregarded.

For the tangential degrees of freedom, there are three different force- and torque-laws to be implemented: (i) friction, (ii) rolling resistance, and (iii) torsion resistance, as described in Luding et al. (2005). The unique feature of this tangential contact model is the fact that a single procedure can be used to compute either sliding, rolling, or torsion resistance. The subroutine needs a velocity as input and returns the respective force or quasi-force. The material parameters for friction involve a static and a dynamic friction coefficient μ_s and μ_d , a tangential elasticity k_t , and a tangential viscous damping γ_t . For rolling and torsion resistance, the prefactors μ_r , and μ_o are used, similar to the friction coefficient – and also a dynamic and a static coefficient with the same ratio as for friction is defined. Furthermore, there is a rolling- and torsion-mode elasticity k_r and k_o , as well as the rolling and torsion-viscous-damping coefficients γ_r and γ_o .

It is important to note that the viscous dissipation takes place in a two-particle contact. In the bulk material, where many particles are in contact with each other, this dissipation mode is very inefficient for long wave length cooperative modes of motion. Therefore, an additional damping with the background can be introduced, so that the force \mathbf{f}_i on particle i is $\mathbf{f}_i = \sum_j (f^n \mathbf{n} + f^t \mathbf{t}) - \gamma_b \mathbf{v}_i$, and the resultant torque is $\mathbf{q}_i = \sum_j \mathbf{q}_i^{\text{friction}} + \mathbf{q}_i^{\text{rolling}} + \mathbf{q}_i^{\text{torsion}} - \gamma_{br} a_i^2 \boldsymbol{\omega}_i$ with the damping artificially enhanced in the spirit of a rapid relaxation and equilibration. Note however, that all viscous forces make the problem rate-dependent, a feature that is studied in more detail elsewhere.

3 Swelling Simulation Results

In this section the results obtained from simulation of a swelling test is presented, where the particles are initially positioned on a square-lattice in a cubic system with periodic boundary conditions, in order to avoid wall effects. The system is first allowed to evolve to a disordered state, by attributing random velocities to all particles. The density is then increased by slowly increasing the particle size while the system volume $V = L^3$, with $L = 0.025$ m, is kept constant. The systems examined in the following contain $N = 1728$ particles with equal radii a . In the

simulations, the radii grow according to the relation $da/dt = g_r a$. The growth is stopped when a target volume fraction v_{\max} , is reached, where the volume fraction is defined as $v = NV(a)/V$, with the particle volume $V(a) = (4/3)\pi a^3$. The particle mass $m(a) = \rho V(a)$, with the fixed material density ρ , changes with the radius during the growth period. The volume fraction changes with time according to the relation $dv/dt = 3v g_r$, which leads to the volume fraction $v = v_0 \exp\{3g_r t\}$ as function of time t . The so called void ratio $e = [V - V(a)]/V(a)$ is related to the volume fraction v as $e = (1/v) - 1$. The model parameters assumed are summarized in Table 1. The particles correspond to spheres with initial radius $a_0 = 5 \mu\text{m}$, growing up to a maximum radius of $a_{\max} = 11.7 \mu\text{m}$ at volume fraction $v_{\max} = 0.75$.

Table 1. Microscopic material parameters according to the contact model in Ref. [7]

Property	Symbol	Values	SI units
Time Unit	t_u	1	1 μs
Length Unit	x_u	1	10 mm
Mass Unit	m_u	1	1 mg
Particle radius	$a(t) = a_0 \exp(g_r t)$		
Initial particle radius	a_0	$5 \cdot 10^{-4}$	$5 \cdot 10^{-6}$ m
Growth rate factor	g_r	0.02	1/s
Material density	ρ	2000	2000 kg/m ³
Elastic stiffness	$k = k_2$	100	10^8 kg/s ²
Plastic stiffness	k_p / k	0.2	
Adhesion "stiffness"	k_a / k	1.0	
Friction stiffness	k_f / k	0.2	
Rolling=Torsion stiffness	$k_r / k = k_t / k$	0.2	
Plasticity range	ϕ_p	0.05	
Coulomb friction coefficient	$\mu = \mu_d = \mu_s$	1	
Rolling=torsion coefficient	$\mu_r = \mu_0$	0.1	
Normal viscosity	$\gamma = \gamma_n$	$2 \cdot 10^{-4}$	$2 \cdot 10^{-4}$ kg/s
Friction viscosity	γ_f / γ	0.25	
Rolling viscosity	$\gamma_r / \gamma = \gamma_0 / \gamma$	0.25	
Torsion viscosity	$\gamma_t / \gamma = \gamma_r / \gamma$	0.25	
Background viscosity	γ_b / γ	0.10	
Background viscous torque	γ_{br} / γ	0.05	

Fig. 1 shows the void ratio e plotted as function of the dimensionless average swelling pressure pd/k_1 , with $d = 2a$ in a semi-logarithmic representation. It is obvious that with an increase of the pressure the void ratio decreases. In particular the curves of Fig. 1a are obtained for different values of the friction coefficient at constant $\mu_r = 0.1$, and the curves of Fig. 1b are obtained for different values of rolling- and torsion-coefficients at constant $\mu = 1$. From Fig. 1a one can conclude that small friction coefficients are always related to rather high densities, i.e.,

small void ratios. Larger and larger friction coefficients, however, are not always sufficient to guarantee a lower and lower packing density, i.e., higher and higher void ratio. The simulations almost collapse for $\mu \geq 1$ (data not shown). From Fig.1b one observes similarly that larger and larger rolling- and torsion- resistance leads to smaller densities, i.e., larger void ratio. It can also be noted that for higher pressures the influence of the friction coefficient and of the rolling- and torsion-coefficients on the void ratio becomes smaller.

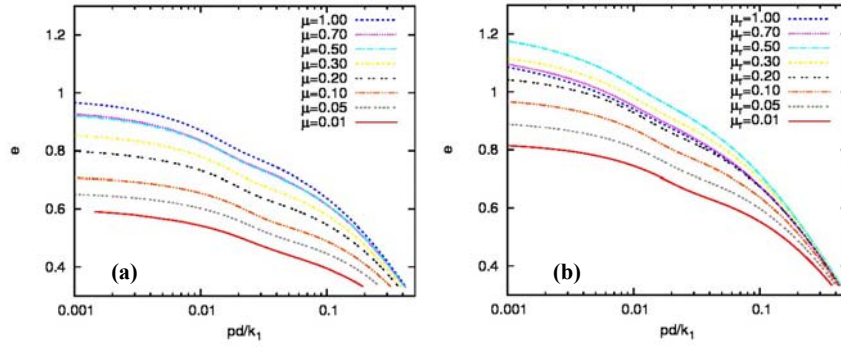


Fig. 1 Void ratio versus dimensionless pressure for different values of the friction coefficient (a), and of the rolling- and torsion-coefficients (b).

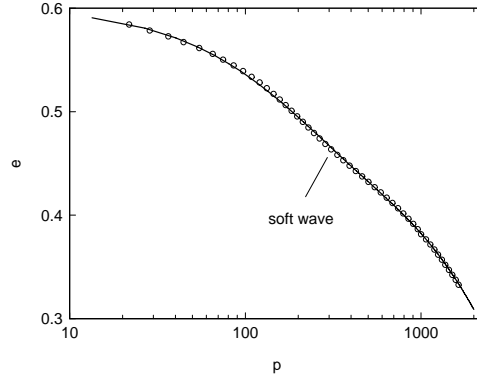


Fig. 2 Void ratio versus pressure; the circles are DEM data, the solid curve is Eq. (2)

For a phenomenological description of the reduction of the void ratio the results obtained from the simulation with the discrete element model (DEM) can be well approximated using the following analytical form proposed by Bauer (2009):

$$e = c_1 \exp\left\{-\frac{p}{h_1}\right\} + c_2 \exp\left\{-\frac{p}{h_2}\right\}. \quad (2)$$

Herein c_1 and c_2 are dimensionless parameters, p is the average pressure, and h_1 and h_2 are parameters with the dimension of stress. For instance for $g_r = 0.02$, $\mu = 0.01$, and $\mu_r = 0.1$ the results from DEM in Fig. 2 can be fitted with the exponential function in Eq. (2) for $c_1 = 0.129$; $h_1 = 179$; $c_2 = 0.472$ and $h_2 = 4717$. It is also of interest to note that Eq. (2) is apt fitting the soft wave transition between the two regimes, as observed at dimensionless pressures $pd/k_1 \approx \phi_f = 0.05$ in the semi-logarithmic representation. Thus, the existence of an elasto-plastic regime for small pressure and a semi-elastic regime for high pressures leads to two regimes, under swelling and isotropic compression, that are well fitted by the analytical form in Eq. (2). The influence of the model parameters on the location of the soft wave will be investigated in more detail in a future publication.

Acknowledgements

Valuable discussions with H.-J. Butt, M. Kappl, J. Tomas, and R. Tykhoniuk are acknowledged. Furthermore, we acknowledge the financial support of the Deutsche Forschungsgemeinschaft (DFG) and the Stichting voor Fundamenteel Onderzoek der Materie (FOM), financially supported by the Nederlandse Organisatie voor Wetenschappelijk Onderzoek (NWO).

References

- Bartels G, Unger T, Kadau D, Wolf DE, Kertesz J (2005) The effect of contact torques on porosity of cohesive powders. *Granular Matter*, 7: 139
- Bauer E (2010) Compression laws for granular materials. Publication in preparation.
- Rapaport DC (1995) *The Art of Molecular Dynamics Simulation*. Cambridge University Press, Cambridge
- Thornton C (2000) Numerical simulations of deviatoric shear deformation of granular media. *Geotechnique*, 50(1):43–53
- Thornton C, Zhang L (2001) A DEM comparison of different shear testing devices. In Y. Kishino, editor, *Powders & Grains 2001*, pages 183–190, Rotterdam, 2001. Balkema.
- Tomas J (2000) Particle adhesion fundamentals and bulk powder consolidation. *KONA*, 18:157–169
- Luding S, Manetsberger K, Müllers J (2005) A discrete model for long time sintering, *Journal of the Mechanics and Physics of Solids* 53(2), 455–491.
- Luding S (2008) Cohesive frictional powders: Contact models for tension. *Granular Matter*, 10:235–246.
- Morgeneyer M, Rock M, Schwedes J, Brendel L, Johnson K, Kadau D, Wolf DE, Heim LO (2006) Compaction and mechanical properties of cohesive granular media. In Walzel P, Linz S, Krülle C., Grochowski R, editors, *Behavior of Granular Media*, pages 107–136. Shaker Verlag, ISBN 3-8322-5524-9
- Oquendo WF, Munoz JD, Lizcano A (2009) Oedometric test, Bauer's law and the micro-macro connection for a dry sand. *Computer Physics Communication*, 180:616–620